Mechanism and Branching Ratios of Hydroxy Ethers + • OH Gas phase Reactions: Relevance of H Bond Interactions

ARTICLE *in* THE JOURNAL OF PHYSICAL CHEMISTRY A · JULY 2010

Impact Factor: 2.69 · DOI: 10.1021/jp103575f · Source: PubMed

3 AUTHORS, INCLUDING:

Annia Galano
Metropolitan Autonomous University
153 PUBLICATIONS **3,371** CITATIONS

SEE PROFILE

Juan Raul Alvarez-Idaboy
Universidad Nacional Autónoma de México
121 PUBLICATIONS **2,177** CITATIONS

SEE PROFILE

Mechanism and Branching Ratios of Hydroxy Ethers + •OH Gas phase Reactions: Relevance of H Bond Interactions

Annia Galano,*,† J. Raul Alvarez-Idaboy,*,‡ and Misaela Francisco-Márquez†

[1] Departamento de Química, Universidad Autónoma Metropolitana-Iztapalapa, San Rafael Atlixco 186, Col. Vicentina, Iztapalapa, C. P. 09340, México D. F. México and [2] Facultad de Química, Departamento de Física y Química Teórica, Universidad Nacional Autónoma de México, México DF 04510, México

Received: April 20, 2010; Revised Manuscript Received: May 29, 2010

A theoretical study on the mechanism and branching ratios of the gas phase reactions of hydroxyl radicals with a series of hydroxy ethers is presented. This is the first report on branching ratios for these reactions. The studied hydroxy ethers are: methoxy-methanol (MM), ethoxy-methanol (EM), 1-methoxy-ethanol (1ME), 2-methoxy-ethanol (2ME), and 2-ethoxy-ethanol (2EE). All the possible H abstraction channels have been modeled, involving the rupture of C−H and O−H bonds. The H abstractions from the alcohol group were found to be almost negligible for all the studied systems. The role of H bond interactions in the transition states (TS) is discussed, as well as the importance of the location of the reaction site with respect to the alcohol and the ether functional groups. TSs with seven-member ring-like structures were found to lead to stronger H bond interactions than TSs with six- and five-member ring-like structures, with the latter leading to the weakest interactions. Kinetic calculations have been performed within the 250−440 K temperature range. Rate coefficients for the reactions of •OH with MM, EM, and 1ME are reported here for the first time. Nonlinear Arrhenius plots were found for all the overall reactions. Negative activation energies at room temperature are proposed for the •OH reactions with EM, 2ME, and 2EE. The excellent agreement with the scarce experimental data available supports the reliability of the data reported here for the first time.

Introduction

Volatile organic compounds (VOCs) are emitted to the atmosphere from anthropogenic and biogenic sources,[1–4] and may also be formed in situ.[5] The oxidation of VOCs leads to the formation of secondary products, which constitutes one of the largest unknowns in the quantitative prediction of the air quality.[6] In fact, it has been established that for modeling and controlling their impact, it is essential to understand the sources of VOC, their distribution, and the chemical transformations they undergo.[6] Hydroxy ethers are widely used solvents, therefore they are likely to be released into the atmosphere. Accordingly, they have been proposed to contribute to the formation of photochemical air pollution in urban and regional areas.[7] However, there is rather scarce information on the atmospheric chemistry of hydroxy ethers, and it all concerns glycol ethers. The most studied ones are 2-methoxy-ethanol (2ME) and 2-ethoxy-ethanol (2EE).

Dagaut et al.[8] measured absolute rate constants for the gas-phase reactions of hydroxyl radicals with a series of glycol ethers by flash photolysis resonance fluorescence (FPRF) technique, at 298 K. They also studied the temperature dependence of the rate coefficient (k) of the •OH reaction with 2ME between 240 and 440 K, and propose the following Arrhenius expression: $k = (4.5 \pm 1.4) \times 10^{-12} \exp[(325 \pm 100)/T]$ cm^3 molecule^{-1} s^{-1}. To the best of our knowledge this is the only previous report on the temperature dependence of a hydroxy ether reaction with •OH. The rate coefficients for the reactions of •OH with 2ME and 2EE were reported to be 1.25×10^{-11} and 1.87×10^{-11} cm^3 molecule^{-1} s^{-1}, respectively. On the basis of their k values, these authors concluded that the reaction with •OH is the most important sink for glycol ethers in the atmosphere, and that photolysis, reaction with NO_3, and reaction with O_3 are negligibly slow by comparison. This conclusion is in agreement with the important role of hydroxyl radicals in the troposphere,[9–12] where it is considered as the dominant reactive species in the degradation of organic compounds during daylight hours.[5]

Dagaut et al.[8] also proposed that the observed negative activation energy can be rationalized in terms of zero or near-zero activation energy associated with hydrogen atom abstraction from weak C−H bonds combined with the inverse temperature dependence of the pre-exponential factor in the Arrhenius expression. However, the alternative explanation of a complex mechanism via hydrogen bonded prereactant complex as proposed by Singleton and Cvetanovic,[13] has not been considered. Later investigations from our group[14] support the second hypothesis for other VOCs. Moreover, the chemical structure of hydroxy ethers is very close to that of dieters, for which it has been proposed that hydrogen bonds in the transition states could be important in the explanation of negative activation energies and branching ratios.[15] H-bonded transition states drop the enthalpies of activation and decrease the entropy of the transition state, which increases the Gibbs free energy of activation. Therefore, the assumption of negative exponent for T in the rate equation is in disagreement with the role of H bonds in lowering the energy of transition states, which has been described for most of the •OH reactions with oxygenated VOCs.

Stemmler et al.[16] also agree that the reaction of glycol ethers with •OH is expected to be their main removal process in the atmosphere. These authors measured the rate coefficients of the reactions of a series of glycol ethers with •OH, relative to those

* To whom correspondence should be addressed. E-mail: agalano@prodigy.net.mx (A. G.), jidaboy@unam.mx (J. R. A.-I.).
† Universidad Autónoma Metropolitana-Iztapalapa.
‡ Universidad Nacional Autónoma de México.

10.1021/jp103575f
Published on Web 06/24/2010

of hexanol and heptanol, at room temperature. These authors reported values of 1.09×10^{-11} and 1.45×10^{-11} cm^3 $molecule^{-1}$ s^{-1} for the reactions of •OH with 2ME and 2EE, respectively. Porter et al.[17] determined the rate coefficients for the reactions of OH radicals with a series of hydroxy ethers, at 298 ± 2 K, using a pulsed laser photolysis resonance fluorescence technique. Their measurements lead to values of 1.14×10^{-11} and 2.12×10^{-11} cm^3 $molecule^{-1}$ s^{-1} for the reactions of •OH with 2ME and 2EE, respectively. Accordingly, it can be stated that for 2ME, the rate coefficients reported to date are in good agreement, while for 2EE the rate value obtained by Stemmler et al.[16] is about 25% lower than those determined by Dagaut et al.[8] and Porter et al.[17]

Regarding the mechanism, there is a general consensus that the products formed from reaction of OH radicals with alcohols and ethers are consistent with hydrogen atom abstraction by •OH from the reactants.[18,19] The •OH reactions with alcohols are expected to occur mainly by H abstractions from C−H sites, but with non-negligible contributions of the O−H sites, particularly for the smaller compounds of the family.[20,21] For the •OH reactions with ethers calculated branching ratios indicate that the presence of the O atom in the vicinity of H abstractions sites increases their reactivity toward •OH radicals.[22] This influence was proposed to be even larger than that of the nature of the carbon site (primary, secondary, tertiary).

To date there are no reports on the branching ratios of the •OH reactions with hydroxy ethers despite that it has been established that branching ratios between different products in multichannel reactions are as important as the overall rate of reaction, in terms of practical applications and in the understanding of the fundamental mechanisms of chemical reactions.[23,24] Therefore, it is the aim of this work to estimate them for the following series of hydroxy ethers: methoxy-methanol (MM), ethoxy-methanol (EM), 1-methoxy-ethanol (1ME), 2-methoxy-ethanol (2ME), and 2-ethoxy-ethanol (2EE). Because there is no kinetic data available for the •OH reaction with MM, EM, and 1ME, it is also our purpose to provide it here. In addition, there is only one study on the temperature dependence of the rate coefficients for the hydroxy ethers + •OH reactions, carried out for 2ME.[8] For that reason it is also our purpose to provide such information for the •OH reactions with all the hydroxy ethers studied in this work. We also intend to elucidate the reasons of negative activation energies, that is, if they are a consequence of the negative dependence of the exponential or pre-exponential factors, as well as the importance of H bond interactions in the transition states.

Computational Details

Full geometry optimizations were performed with the Gaussian 03[25] program using the 6-311++G(d,p) basis set and the BHandHLYP[26] hybrid HF-density functional. The energies of all the stationary points were improved by single-point calculations using the CCSD(T)[27] method and the same basis set mentioned above. On the basis of our previous experience,[28] the use of CCSD(T)//BHandHLYP approach properly describes the energetic and kinetics features of VOCs + •OH hydrogen abstraction reactions. In addition, for this kind of reactions it has been proven that the differences in geometries between BHandHLYP compared to CCSD and QCISD are minimal.[29] Unrestricted calculations were used for open shell systems. Frequency calculations were carried out for all the stationary points at the DFT level of theory and local minima and transition states were identified by the number of imaginary frequencies (NIMAG = 0 or 1, respectively). Intrinsic Reaction Coordinate (IRC)[30] calculations were carried out at the BH and HLYP/6-311G++(d,p) level of theory to confirm that the transition states structures connect the proper reactants and products. The paths have been computed by following the Gonzalez−Schlegel steepest descent path,[31] in mass-weighted internal coordinates. Fifty points were modeled on each side of the saddle points, with a gradient step size of 0.02 $amu^{1/2}$ bohr. Thermodynamic corrections were included in the calculations of relative energies. The rate constants (k) were calculated using conventional transition state theory (TST).[32–34] The tunneling correction, defined as the Boltzmannn average of the ratio of the quantum and the classical probabilities, were calculated using the Eckart barrier.[35]

Counterpoise corrections (CP) to the basis set superposition error have not been included, since it has been recently demonstrated, for a large variety of systems, that CP corrected energies systematically differ to a larger extent, from the CBS-extrapolated values, than the uncorrected ones,[36] at least when wave function methods are used.

The rate constant for each individual channel has been calculated, according to the conventional transition state theory (TST) and using 1 M standard state as:

$$k = \sigma\kappa\frac{k_B T}{h}e^{-(\Delta G^{\ddagger})/RT} \qquad (1)$$

where k_B and h are the Boltzman and Planck constants; $\Delta G^{\ddagger}$ is the Gibbs free energy of activation; σ represents the reaction path degeneracy, accounting for the number of equivalent reaction paths; and κ accounts for tunneling corrections. It has been assumed that neither mixing nor crossover between different pathways occurs. Thus, the overall rate coefficient (k) corresponding to the reaction of •OH with each hydroxy ether is calculated as the sum of the rate coefficients of each channel.[37]

Numerous reports on the mechanism of •OH reactions with VOCs have proposed the presence of reactant complexes (RC) in the entrance channel. For hydroxy ethers (HE) such mechanism corresponds to:

$$HE + {}^{\bullet}OH \underset{k_{-1}}{\overset{k_1}{\rightleftharpoons}} RC \xrightarrow{k_2} \text{product} + H_2O \qquad (m1)$$

The steady state approximation can be used, when such mechanism is involved, if the reactant complex does not accumulate, that is, if $(k_{-1} + k_2) > k_1$. In fact for most atmospheric reactions, including those of HE + •OH, the enthalpy of complexation is smaller than the associated entropy loss. Therefore, the reactant complex has higher Gibbs free energy than the isolated reactants (Figure 1). It means that $K_P < 1$, and since this equilibrium constant corresponds to the ratio k_1/k_{-1} it becomes obvious that $k_{-1} > k_1$. Therefore, the steady state applies, regardless of the k_2 value.

According to this approximation the rate constant for any reaction path taking place through the reaction mechanism m_1 can be expressed as:

$$k = \frac{k_1 k_2}{k_{-1} + k_2} \qquad (2)$$

This equation has two limit cases. The first one is for $k_{-1} \gg k_2$, that is, the barrier of the second step is considerably larger (by

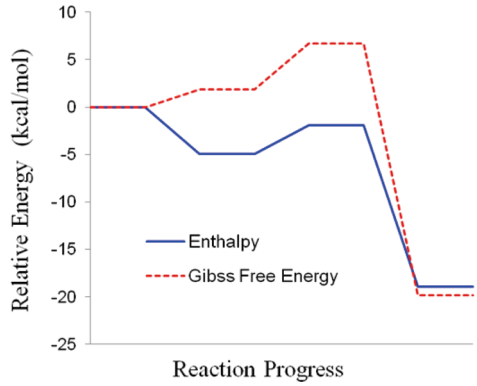

Figure 1. Energy profiles in terms of entalpies and Gibbs free energies, using one of the paths of the •OH + EM reaction, as an example.

2 kcal/mol or more) than that of the reverse first-step. In this case, eq 2 becomes:

$$k = \frac{k_1 k_2}{k_{-1}} = K_1 k_2 \tag{3}$$

where K_1 is the equilibrium constants of the first steep of mechanism m1, that is, the formation of the reactant complex. In this case the second step is the rate determining step (RDS). This limit case corresponds to the reactions studied in the present work.

Since the equilibrium constant (K_1) and the rate constant of the second step (k_2) can be calculated as:

$$K_1 = \mathrm{e}^{-(G_{RC}-G_{reac})/RT} \tag{4}$$

$$k_2 = \frac{k_B T}{h}\mathrm{e}^{-(G_{TS}-G_{RC})/RT} \tag{5}$$

Equation 3 can be rewritten as:

$$k = \mathrm{e}^{-(G_{RC}-G_{reac})/RT}\frac{k_B T}{h}\mathrm{e}^{-(G_{TS}-G_{RC})/RT} \tag{6}$$

It is evident from eq 6 that the term G_{RC} cancels out and the total classical rate constant becomes:

$$k = \frac{k_B T}{h}\mathrm{e}^{-(G_{TS}-G_{reac})/RT} \tag{7}$$

which is pressure independent. However, when there is a possibility of quantum mechanical tunneling there are two limit cases related to the pressure dependence. At high pressure limit a thermal equilibrium distribution of energy levels is assumed and all energy levels from the bottom of the well of the complex up to the barrier might contribute to tunneling. Therefore, the tunnelling correction (κ) becomes larger due to the collisional stabilization of the RC. On the contrary, at low pressure limit the lack of collisional stabilization causes that none of the reactant complexes can reach energies below reactants, and κ value is the same as when tunneling is calculated from the isolated reactants. Accordingly the difference between high and low pressure limit rate constants arise from the value of κ. Such differences are rather small and usually below the expected

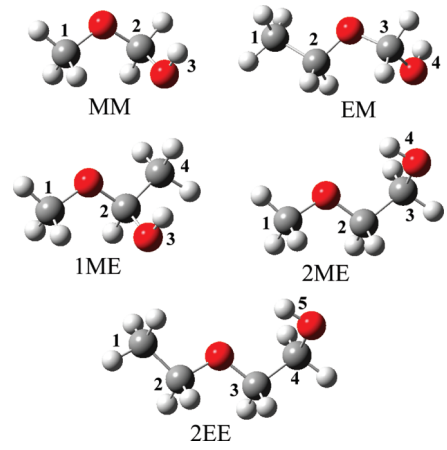

Figure 2. Hydroxy ethers and site numbers used in this work. Methoxy-methanol (MM), ethoxy-methanol (EM), 1-methoxy-ethanol (1ME), 2-methoxy-ethanol (2ME), and 2-ethoxy-ethanol (2EE).

accuracy of rate constant calculations. In the present case we assumed low pressure limit for tunneling correction because there is a better agreement with experiment. However, the mechanistic conclusions would be the same if the high pressure limit is assumed. Alternative explanations on the use of steady state approximation for this kind of reactions can be found elsewhere.[38]

Results and Discussion

The OH radical reactions with five different hydroxy ethers have been studied in the present work. The sites of reaction have been labeled to facilitate discussion (Figure 2). Every possible H abstraction path has been considered:

Methoxy-methanol (MM):

$$CH_3OCH_2OH + {}^{\bullet}OH \rightarrow {}^{\bullet}CH_2OCH_2OH \quad \text{(MM-1)}$$

$$CH_3OCH_2OH + {}^{\bullet}OH \rightarrow CH_3O{}^{\bullet}CHOH \quad \text{(MM-2)}$$

$$CH_3OCH_2OH + {}^{\bullet}OH \rightarrow CH_3OCH_2O^{\bullet} \quad \text{(MM-3)}$$

Ethoxy-methanol (EM):

$$CH_3CH_2OCH_2OH + {}^{\bullet}OH \rightarrow {}^{\bullet}CH_2CH_2OCH_2OH \quad \text{(EM-1)}$$

$$CH_3CH_2OCH_2OH + {}^{\bullet}OH \rightarrow CH_3{}^{\bullet}CHOCH_2OH \quad \text{(EM-2)}$$

$$CH_3CH_2OCH_2OH + {}^{\bullet}OH \rightarrow CH_3CH_2O{}^{\bullet}CHOH \quad \text{(EM-3)}$$

$$CH_3CH_2OCH_2OH + {}^{\bullet}OH \rightarrow CH_3CH_2OCH_2O^{\bullet} \quad \text{(EM-4)}$$

1-methoxy-ethanol (1ME):

$$CH_3OCH(OH)CH_3 + {}^{\bullet}OH \rightarrow {}^{\bullet}CH_2OCH(OH)CH_3 \quad (1ME\text{-}1)$$

$$CH_3OCH(OH)CH_3 + {}^{\bullet}OH \rightarrow CH_3O{}^{\bullet}C(OH)CH_3 \quad (1ME\text{-}2)$$

$$CH_3OCH(OH)CH_3 + {}^{\bullet}OH \rightarrow CH_3OCH({}^{\bullet}O)CH_3 \quad (1ME\text{-}3)$$

$$CH_3OCH(OH)CH_3 + {}^{\bullet}OH \rightarrow CH_3OCH(OH){}^{\bullet}CH_2 \quad (1ME\text{-}4)$$

2-methoxy-ethanol (2ME):

$$CH_3OCH_2CH_2OH + {}^{\bullet}OH \rightarrow {}^{\bullet}CH_2OCH_2CH_2OH \quad (2ME\text{-}1)$$

$$CH_3OCH_2CH_2OH + {}^{\bullet}OH \rightarrow CH_3O{}^{\bullet}CHCH_2OH \quad (2ME\text{-}2)$$

$$CH_3OCH_2CH_2OH + {}^{\bullet}OH \rightarrow CH_3OCH_2{}^{\bullet}CHOH \quad (2ME\text{-}3)$$

$$CH_3OCH_2CH_2OH + {}^{\bullet}OH \rightarrow CH_3OCH_2CH_2O{}^{\bullet} \quad (2ME\text{-}4)$$

2-ethoxy-ethanol (2EE):

$$CH_3CH_2OCH_2CH_2OH + {}^{\bullet}OH \rightarrow {}^{\bullet}CH_2CH_2OCH_2CH_2OH \quad (2EE\text{-}1)$$

$$CH_3CH_2OCH_2CH_2OH + {}^{\bullet}OH \rightarrow CH_3{}^{\bullet}CHOCH_2CH_2OH \quad (2EE\text{-}2)$$

$$CH_3CH_2OCH_2CH_2OH + {}^{\bullet}OH \rightarrow CH_3CH_2O{}^{\bullet}CHCH_2OH \quad (2EE\text{-}3)$$

$$CH_3CH_2OCH_2CH_2OH + {}^{\bullet}OH \rightarrow CH_3CH_2OCH_2{}^{\bullet}CHOH \quad (2EE\text{-}4)$$

$$CH_3CH_2OCH_2CH_2OH + {}^{\bullet}OH \rightarrow CH_3CH_2OCH_2CH_2O{}^{\bullet} \quad (2EE\text{-}5)$$

Due to the presence of the O atoms in the hydroxy ethers structures not all the H, attached to the same carbon, are equivalent. The difference arises from the H arrangement with respect to the O atoms, which promotes or prevents the formation of H bond interactions in the transition states (TS) structures. Therefore, each reaction path, mentioned above, can proceed in more than one way (channel of reaction). This peculiarity of H abstractions from oxygenated organic compounds has been previously taken into account and accordingly applied for the ${}^{\bullet}OH$ reactions with ketones and ethers.[22,39,40]

The fully optimized structures of the TSs are shown in Figures 3−7. For path 1 of the MM + ${}^{\bullet}OH$ reaction there are two possible transition states, one of them (MM-TS1H) with a H bond interaction between the H atom in the ${}^{\bullet}OH$ radical and the O atom in the hydroxyl moiety of MM. The other TS (MM-TS1, Figure 3) does not present such interaction, suggesting that its energy should be higher than that of MM-TS1H. TSs corresponding to the H abstractions from sites 2 and 3 also present H bond interactions, involving the H atom in the ${}^{\bullet}OH$ radical and the O atom in the ether group of MM.

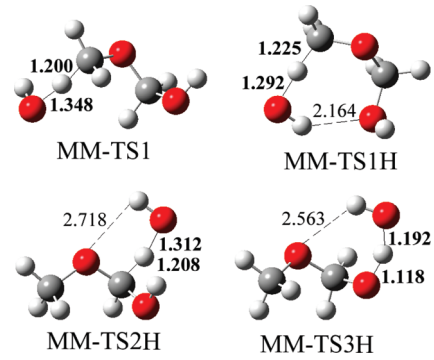

Figure 3. Optimized geometries of the transitions states for the ${}^{\bullet}OH$ + MM channels of reaction. Distances are in Å.

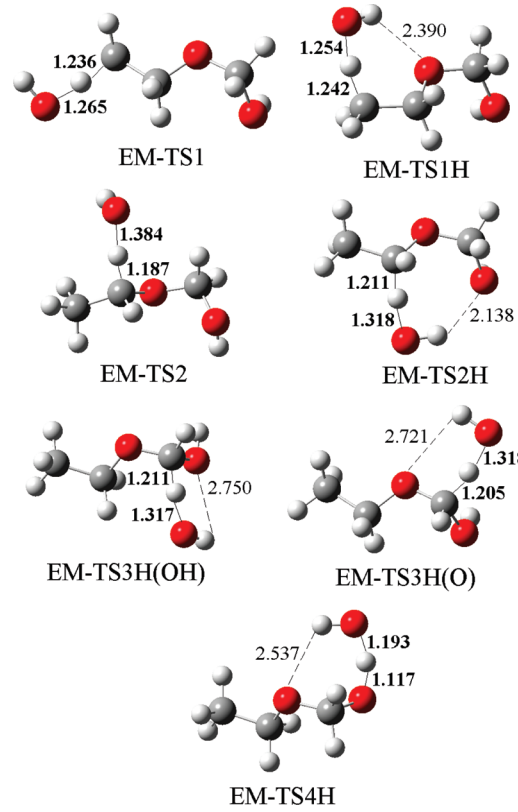

Figure 4. Optimized geometries of the transitions states for the ${}^{\bullet}OH$ + EM channels of reaction. Distances are in Å.

For the reaction of ${}^{\bullet}OH$ with EM seven TS structures were located. Two different TS have been identified for H abstractions from sites 1, 2, and 3. For path 1 and 2 there is one TS presenting H bond interaction and one TS without it (Figure 4). For path 3, on the other hand, both TS present such interaction. However, due to the double functionality of hydroxy ethers, one of them involves the alcohol group (EM-TS3H(OH)) and the other the ether group (EM-TS3H(O)) in EM. According to the geometrical parameters shown in Figure 4, the interaction with the ether group is expected to be slightly stronger than that with the alcohol group.

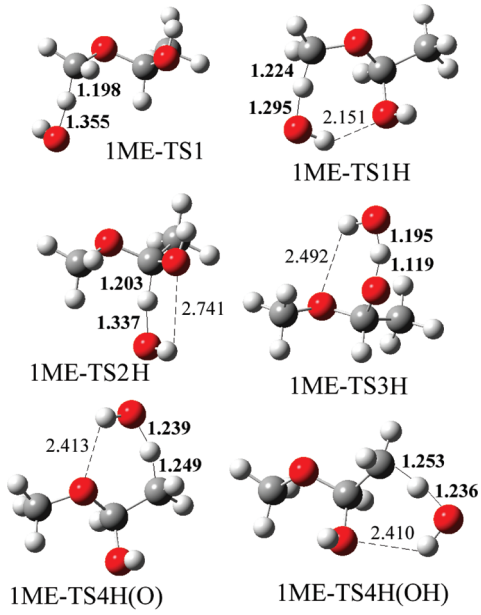

Figure 5. Optimized geometries of the transitions states for the •OH + 1ME channels of reaction. Distances are in Å.

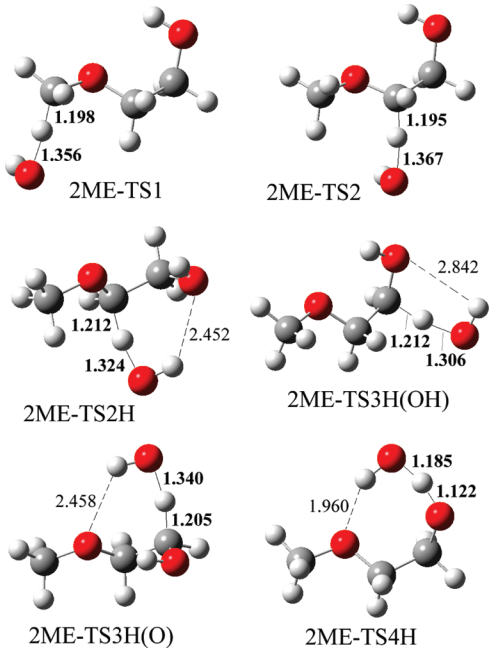

Figure 6. Optimized geometries of the transitions states for the •OH + 2ME channels of reaction. Distances are in Å.

Six different transition states were located for the •OH + 1ME reaction (Figure 5). Only one TS structure was found for paths 2 and 3, both of them presenting H bond interaction, involving the alcohol and ether group for 1ME-TS2H and 1ME-TS3H, respectively. For paths 1 and 4, on the other hand, there are two TS structures connecting reactants and products. Those corresponding to path 1 differentiate by the absence (1ME-TS1) or presence (1ME-TS1H) of H bond interaction. In contrast, both TSs corresponding to path 4 present this kind of interaction. However, whereas it involves the ether group in 1ME-TS4H(O), it is formed with the alcohol group in 1ME-TS4H(OH). In this particular case both d(H···O) distances are very similar, suggesting that the interactions are of similar strength.

For the •OH + 2ME reaction six TS structures were identified. For reaction paths 1 and 4 only one TS was located. That of

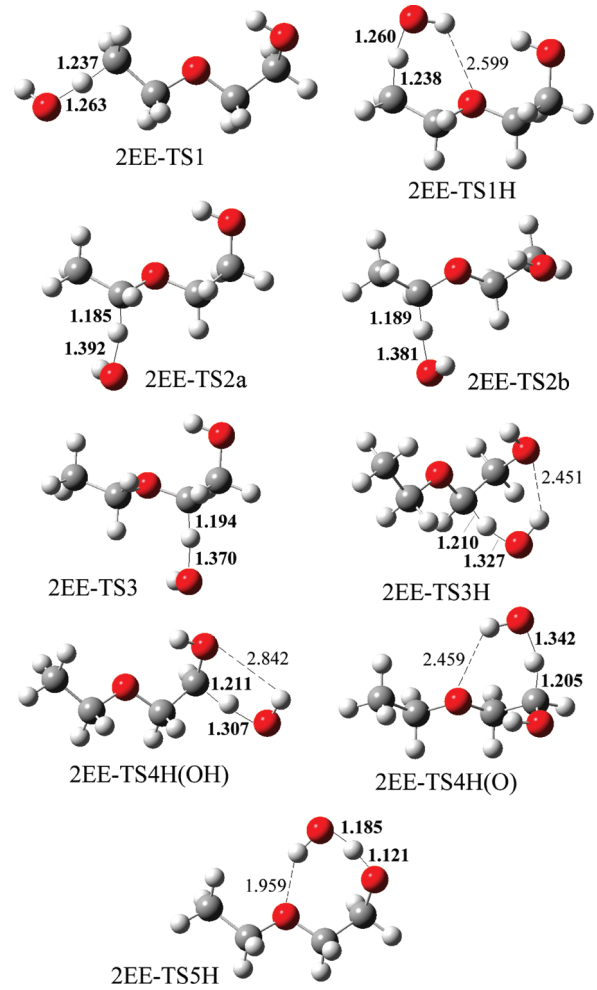

Figure 7. Optimized geometries of the transitions states for the •OH + 2EE channels of reaction. Distances are in Å.

path 1 (2ME-TS1) does not show any H bond interaction, every attempt to find a H-bonded structure invariably evolved to structures where the H in the OH radical moiety is far enough from the O atoms in 2ME to prevent the interactions. The TS for path 4, on the other hand shows a strong H bond interaction (d(H···O) = 1.96 Å, Figure 6) between the H in the •OH and the ether group in 2ME. For path 2, two transition states have been located, one of them with no H bond interaction, and the other forming a hydrogen bond between the H in the •OH radical and the alcohol group in 2ME. For path 3, two transition states have been also located, but in this case both of them show intermolecular interactions. In 2ME-TS3H(OH) the interaction involves the alcohol group in 2ME, whereas in 2ME-TS3H(O) it involves the O atom of the ether group. On the basis of the d(H···O) distances the interaction with the ether group is stronger than that involving the alcohol group.

Nine different transition states were found for the •OH + 2EE reaction. In this case for all the abstraction sites, with the logical exception of site 5 where there is only one H, two transition states have been identified. There are two TS structures for paths 1 and 3, one of them with H bond interaction and the other without it. For path 4, on the other hand, both transition states show H bond interaction. It involves the ether group in 2EE-TS4H(O) and the alcohol group in 2EE-TS4H(OH). Similarly to what was discussed for 2ME, the interaction with the ether group is stronger than that involving the alcohol group, since the d(H···O) distance is about 0.4 Å shorter. For path 2 none of the located TSs has H bond interactions.

TABLE 1: Energies of Relevant Stationary Points, Relative to Isolated Reactants, in kcal/mol, for the •OH + MM Reaction

	ΔE^a			ΔH			ΔG		
channel	CR	TS	Prod.	CR	TS	Prod.	CR	TS	Prod.
1	−5.22	1.41	−17.45	−5.60	0.61	−17.14	1.16	9.12	−18.17
1H	−4.83	0.13	−17.45	−5.22	−1.01	−17.14	1.64	8.60	−18.17
2H	−5.68	0.73	−19.67	−6.26	0.06	−19.23	1.95	8.44	−20.59
3H	−5.68	3.65	−9.60	−6.26	2.74	−9.39	1.95	11.69	−10.39

[a] Including ZPE corrections.

TABLE 2: Energies of Relevant Stationary Points, Relative to Isolated Reactants, in kcal/mol, for the •OH + EM Reaction

	ΔE^a			ΔH			ΔG		
channel	CR	TS	Prod.	CR	TS	Prod.	CR	TS	Prod.
1	−5.85	4.50	−11.15	−6.42	3.96	−10.46	1.84	11.63	−12.37
1H	−5.85	2.50	−11.15	−6.42	1.55	−10.46	1.84	10.71	−12.37
2	−4.95	−0.17	−18.97	−5.32	−0.84	−18.56	1.50	7.62	−19.83
2H	−4.95	−1.96	−18.97	−5.32	−2.98	−18.56	1.50	6.72	−19.83
3H(OH)	−4.95	0.55	−19.70	−5.32	−0.06	−19.26	1.50	8.37	−20.63
3H(O)	−5.85	0.47	−19.70	−6.42	−0.18	−19.26	1.84	8.24	−20.63
4H	−5.85	3.45	−9.73	−6.42	2.55	−9.50	1.84	11.50	−10.50

[a] Including ZPE corrections.

TABLE 3: Energies of Relevant Stationary Points, Relative to Isolated Reactants, in kcal/mol, for the •OH + 1ME Reaction

	ΔE^a			ΔH			ΔG		
channel	CR	TS	Prod.	CR	TS	Prod.	CR	TS	Prod.
1	−4.90	1.18	−18.60	−5.30	0.40	−18.14	1.72	8.90	−19.53
1H	−5.37	−0.22	−18.60	−5.76	−1.33	−18.14	1.25	8.30	−19.53
2H	−5.05	−0.79	−18.90	−5.40	−1.37	−18.43	1.39	7.19	−19.99
3H	−5.73	3.63	−10.75	−6.25	2.74	−10.57	1.85	11.91	−11.55
4H(O)	−5.37	3.09	−10.19	−5.76	2.21	−9.63	1.25	11.24	−11.32
4H(OH)	−5.05	3.71	−10.19	−5.40	2.83	−9.63	1.39	11.87	−11.32

[a] Including ZPE corrections.

TABLE 4: Energies of Relevant Stationary Points, Relative to Isolated Reactants, in kcal/mol, for the •OH + 2ME Reaction

	ΔE^a			ΔH			ΔG		
channel	CR	TS	prod.	CR	TS	prod.	CR	TS	prod.
1		1.12	−16.67		0.39	−16.09		8.74	−17.83
2	−5.54	1.02	−16.74	−5.92	0.31	−16.08	0.66	8.56	−18.09
2H	−5.54	−0.10	−16.74	−5.92	−0.68	−16.08	0.66	7.57	−18.09
3H(OH)	−5.54	−1.92	−16.77	−5.92	−2.78	−16.21	0.66	6.34	−17.93
3H(O)	−4.35	1.93	−16.77	−4.69	1.36	−16.21	2.32	9.62	−17.93
4H	−5.67	−0.76	−9.56	−6.29	−1.61	−9.32	2.26	7.43	−10.40

[a] Including ZPE corrections.

Relative energies of the stationary points involved in every reaction path, with respect to the isolated reactants, are reported in Tables 1−5, and the reaction profiles have been plotted in Figure 8 including ZPE corrections. All the reaction paths were found to be exothermic and exergonic, indicating that they are all viable chemical processes. The reaction profiles of all the studied channels of reaction are shown in Figure 8. As these profiles show, there is a reactant complex associated with most of the reaction channels. Their optimized structures are provided as Supporting Information (Figures 1S−5S).

For all the studied •OH + hydroxy ethers reactions the channel with the lowest barrier always involves a TS that presents H bond interactions. Therefore, such interactions do not only lower the energy of the TSs, but also seem to play an important role on the reactivity of the studied VOCs. For the •OH reaction with MM H abstraction from site 1, involving the transition state MM-TS1H, was found to be the channel with the lowest barrier (Table 1), followed by H abstraction from site 2 (MM-TS2H). The *d*(H···O) in MM-TS1H is significantly shorter than in MM-TS2H (about 0.55 Å), indicating a stronger H bond interaction in the MM-TS1H. For the •OH + EM reaction the lowest barrier corresponds to path 2 and involves the transition state EM-TS2H. This TS is also the one with the shortest *d*(H···O) associated with the H bond interaction. For the •OH + EM reaction, on the other hand, the lowest barrier does not correspond to the channel involving the TS with the strongest H bond (1ME-TS1H) but to the abstraction from site 2 (Table 2). 1ME-TS2H also has this kind of interaction but with the *d*(H···O) distance 0.59 Å longer. This indicates that the difference in nature between sites 1 and 2 in 1ME affects the site reactivity to a larger extent than the strength of the H bond interaction. Site 2 of 1ME is the only site, among all the studied ones, corresponding to a tertiary carbon, which in this particular case has the additional characteristic of being bonded to the two O atoms of this hydroxy ether. Such location seems to be responsible for the large reactivity of this site.

For the •OH reactions with 2ME and 2EE the strongest H bond interaction is present in the transition states corresponding

TABLE 5: Energies of Relevant Stationary Points, Relative to Isolated Reactants, in kcal/mol, for the •OH + 2EE Reaction

	ΔE^a			ΔH			ΔG		
channel	CR	TS	prod.	CR	TS	prod.	CR	TS	prod.
1		4.49	−13.47		3.97	−12.93		11.69	−14.55
1H	−4.90	3.34	−13.47	−5.27	2.56	−12.93	2.07	11.19	−14.55
2a	−4.90	−0.37	−20.18	−5.27	−0.99	−19.72	2.07	7.34	−21.24
2b	−5.57	−0.47	−20.18	−5.95	−1.10	−19.72	0.64	7.28	−21.24
3	−4.90	−0.21	−18.83	−5.27	−0.78	−18.30	2.07	7.47	−20.06
3H	−5.57	−2.04	−18.83	−5.95	−2.89	−18.30	0.64	6.25	−20.06
4H(OH)	−5.57	1.83	−19.73	−5.95	1.28	−19.42	0.64	9.53	−20.54
4H(O)	−4.90	−0.91	−19.73	−5.27	−1.75	−19.42	2.07	7.29	−20.54
5H	−5.79	2.51	−9.59	−6.42	1.42	−9.36	2.24	11.16	−10.40

[a] Including ZPE corrections.

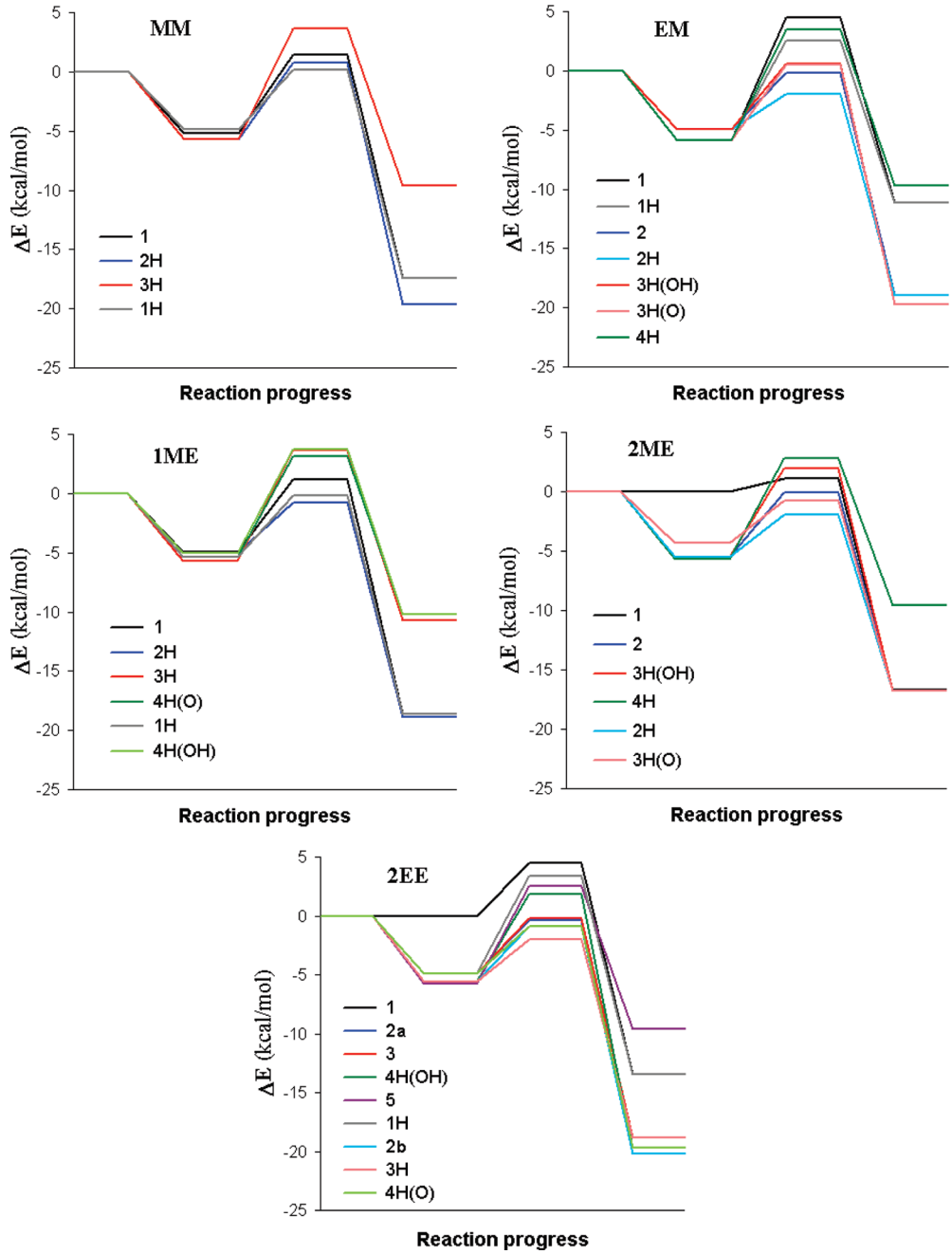

Figure 8. Reaction profiles including ZPE corrections.

to H abstractions from the alcohol group of the hydroxy ethers, that is, in 2ME-TS4H and 2EE-TS5H, respectively. However, since they correspond to H abstractions from O−H sites, that are stronger bonds than the C−H ones, they are not among the channels with lower energy barriers. It was found that the channels with lowest barriers are those involving 2ME-TS2H and 2EE-TS3H, for 2ME and 2 EE, respectively (Tables 4 and 5). In both cases the site of reaction with the lowest barrier

TABLE 6: Calculated and Experimental Rate Coefficients ($\times 10^{11}$, cm^3 molecule^{-1} s^{-1}) at 298 K

	MM	EM	1ME	2ME	2EE
calculated	0.096	0.413	0.194	0.833	1.11
experimental				1.25[a]	1.87[a]
				1.08[b]	1.45[b]
				1.41[c]	1.74[c]
				1.14[d]	2.12[d]

[a] Reference 8 (flash photolysis resonance fluorescence). [b] Reference 16 (relative rate). [c] Reference 17 (relative rate). [d] Reference 17 (pulsed laser photolysis laser-induced fluorescence).

TABLE 7: Branching Ratios for the Different Channels Contributing to the •OH Reactions with the Studied Hydroxy Ethers, at 298 K

MM	EM	1ME	2ME	2EE
$\Gamma_1 = 13.21$	$\Gamma_1 = 0.19$	$\Gamma_1 = 8.55$	$\Gamma_1 = 9.71$	$\Gamma_1 = 0.06$
$\Gamma_{1H} = 26.06$	$\Gamma_{1H} = 1.06$	$\Gamma_{1H} = 21.66$	$\Gamma_2 = 8.52$	$\Gamma_{1H} = 0.22$
$\Gamma_{2H} = 59.42$	$\Gamma_2 = 15.96$	$\Gamma_{2H} = 67.76$	$\Gamma_{2H} = 69.66$	$\Gamma_{2a} = 9.51$
$\Gamma_{3H} = 1.31$	$\Gamma_{2H} = 72.65$	$\Gamma_{3H} = 0.46$	$\Gamma_{3H(OH)} = 1.00$	$\Gamma_{2b} = 10.39$
	$\Gamma_{3H(OH)} = 4.30$	$\Gamma_{4H(OH)} = 0.29$	$\Gamma_{3H(O)} = 10.96$	$\Gamma_3 = 7.63$
	$\Gamma_{3H(O)} = 5.46$	$\Gamma_{4H(O)} = 1.28$	$\Gamma_{4H} = 0.15$	$\Gamma_{3H} = 60.91$
	$\Gamma_{4H} = 0.38$			$\Gamma_{4H(OH)} = 0.77$
				$\Gamma_{4H(O)} = 10.35$
				$\Gamma_{5H} = 0.14$

corresponds to the secondary C atoms next to the ether group, and in β position with respect to the alcohol group of the hydroxy ethers. These findings suggest that the effect of the vicinity of the ether group on the reactivity of hydroxy ethers toward •OH radicals is larger than that of the alcohol group.

The calculated values of the overall rate coefficients at 298 K are reported in Table 6, together with the available experimental data. The overall rate coefficient (k) corresponding to the reaction of •OH with each hydroxy ether, is calculated as:

$$k_{MM} = k_1 + k_{1H} + k_{2H} + k_{3H} \quad (8)$$

$$k_{EM} = k_1 + k_{1H} + k_2 + k_{2H} + k_{3H(OH)} + k_{3H(O)} + k_{4H} \quad (9)$$

$$k_{1ME} = k_1 + k_{1H} + k_{2H} + k_{3H} + k_{4H(OH)} + k_{4H(O)} \quad (10)$$

$$k_{2ME} = k_1 + k_2 + k_{2H} + k_{3H(OH)} + k_{3H(O)} + k_{4H} \quad (11)$$

$$k_{2EE} = k_1 + k_{1H} + k_{2a} + k_{2b} + k_3 + k_{3H} + k_{4H(OH)} + k_{4H(O)} + k_{5H} \quad (12)$$

The highest rate coefficient for the reactions of •OH with the presented hydroxy ethers was found to be that of 2EE, and the smallest one corresponds to MM. This seems to be a logical finding based on the size of the studied VOCs. The agreement between the calculated overall rate coefficients and the available experimental data is excellent. The largest discrepancy for the •OH + 2ME reaction was found with the results by Porter et al.,[17] with the calculated k being 1.7 times lower than the experimental value, obtained from relative rate measurements, and the best agreement was obtained with the value reported by Stemmler et al.[16] In this case our rate constant was found to be 1.3 times lower than the experimental one. For the •OH + 2EE reaction the largest discrepancy also arise from comparison with the results by Porter et al.,[17] but in this case when pulsed laser photolysis laser-induced fluorescence was used. The calculated k was found to be 1.9 times lower than the experimental one. The best agreement occurs again with the value reported by Stemmler et al.,[16] with our k being 1.3 times lower than the experimental value. Therefore, the differences between our results and those by Stemmler et al. are not only very small but are also systematic.

The branching ratios, at 298 K, are reported in Table 7. They have been calculated as:

$$\Gamma_i = \frac{k_i}{k_{overall}} \times 100 \quad (13)$$

where k_i represents the rate constant of the i channel of reaction.

According to our results, the main path of the •OH + MM reaction is the H abstraction from site 2, contributing ~59% to the overall process. H abstractions from the methyl group are also significant with a contribution of about 38%, which is surprisingly high for a primary C site. The OH site is only a minor path (1.3%), which is in line with the higher strength of the O−H bond, compared to the C−H ones. As the temperature increases the contributions of channel 1H become smaller, whereas those of the other channels increase. However, there are only small variations on the branching ratios within the 250−440 K temperature range (Table 1S, Supporting Information). Site 2 in MM corresponds to a secondary carbon atom, which in addition is in α position with respect to both functional groups in this hydroxy ether. All these characteristics contribute to the highest reactivity of this site.

For the •OH + EM reaction the differences in branching ratio are more dramatic. H abstractions from site 2 in this case contribute 88.6% to the overall process. In addition, the role of the H bond in transition state EM-TS2H is very significant and causes the contribution of channel 2H to be four times larger than that of channel 2. The second major path corresponds to H abstractions from site 3, contributing 9.8% to the overall rate coefficient at room temperature. In this case both transition states, EM-TS3H(OH) and EM-TS3H(O), present H bond interactions; however, based on the branching ratios of both channels, the increase on reactivity is larger when it involves the O atom in the ether group. As the temperature increases the

contributions from path 3 to the overall rate coefficients become more important, reaching 26% at 440 K (Table 2S). It is interesting to notice that sites 2 and 3 both correspond to secondary C. However, the C atom in site 2 is in α position with respect to the ether group, whereas the C atom in site 3 is in α position with respect to both the ether and the alcohol groups. Therefore, the location of the reaction site with respect to the functional groups determines the difference of reactivity in this case. On the basis of only structure−activity relationship considerations, the finding that site 2 is more reactive than site 3, toward OH radical might seem illogical. However, it can be explained based on the structure of the involved transition states. H bond interactions present in the TS structures play a crucial role in this case. Whereas in EM-TS2H the d(H···O) distance is 2.138 Å, in both EM-TS3H(OH) and EM-TS3H(O) this distance is about 0.6 Å longer. This difference is caused by the molecular arrangements. EM-TS2H has a seven-member ring-like structure while EM-TS3H(OH) and EM-TS3H(O) have five-member ring-like structures that prevent the interacting atoms from being as close as in EM-TS2H.

The major path for the 1ME + •OH reaction was found to be path 2, contributing 67.8% to the overall rate coefficient at 298 K. As the temperature increases such contribution decreases, ranging from 70% at 250 K to 62% at 440 K (Table 3S). These branching ratios are not as large as would be expected based on the fact that this site corresponds to a tertiary atom in α position with respect to both the ether and the alcohol groups. This can be explained by the H bonds in the corresponding TS structures. Even though 1ME-TS2 presents a H bond interaction, it has the largest d(H···O) distance, that is, it is the weakest interaction. Therefore, the energy lowering in the other H bonded TSs is larger and increases the branching ratios of those channels. In fact, the second major channel within the studied temperature range is that involving H abstractions from the primary C atom that is in α position with respect to the ether group and in γ position with respect to alcohol group. The contributions of path 1 to the overall rate coefficient were found to vary from 28% at 250 K to 33% at 440 K. Moreover, at all the studied temperature this relative large contribution are mainly due to channel 1H, which involves the TS structure with the strongest H bond for this hydroxy ether (1ME-TS1H). The difference in the strength of the H bond interactions in the TS structures is caused by the position of the H abstraction sites within the hydroxy ether. Apparently, when the TS has a seven-member ring-like structure (1ME-TS1H) it arranges in such a way that the interacting atoms can be located very closely (d(H···O) = 2.15 Å). On the contrary, a five-member ring-like structure (1ME-TS2H) prevents the interacting atoms from getting closer in the TS, which leads to d(H···O) ∼ 2.7 Å. For those TS with six-member ring-like structure (1ME-TS3H, 1ME-TS4H(O) and 1ME-TS4H(OH)) the distance between the interacting atoms is intermediate (d(H···O) ∼ 2.4 Å).

H abstractions from site 2 were found to be the major path of the 2ME + •OH reaction, contributing 78.2% to the overall reaction at 298 K. The influence of temperature on the branching ratios was found to be more significant in this case than for the hydroxy ethers previously analyzed. As the temperature increases the contributions of path 2 decrease from 86% at 250 K to 59% at 440 K (Table 4S). Path 4 was found to contribute the least to the overall rate coefficient, despite of the fact that it has the strongest H bond interaction. This is a logical finding since the O−H bond is significantly stronger than the C−H bonds. Because the strength of the H bond interactions in 2ME-TS2H and 2ME-TS3H(O) are very similar, based on the values of the d(H···O) distances, and both sites correspond to secondary C atoms, the higher reactivity of site 2 can not be explained by these structural features. For this particular hydroxy ether site 2 is an α site with respect to ether group and a β site with respect to the alcohol group, while site 3 is α with respect to the alcohol group and β with respect to the ether group. Therefore, it seems that the vicinity to the ether group increases the site reactivity to a larger extent than the vicinity to the alcohol group. Moreover, the difference in location with respect to both functional groups seems to be the factor influencing the most the relative site reactivity for this particular hydroxy ether.

TABLE 8: Arrhenius Parameters for the Studied Reactions between OH Radical and Hydroxy Ethers at the 250−440 K Temperature Range

	A (cm^3 $mlecule^{-1}$ s^{-1})	E_a (kcal/mol)
MM	5.33×10^{-12}	0.99
EM	1.40×10^{-12}	−0.68
1ME	3.15×10^{-12}	0.27
2ME	3.84×10^{-12}	−0.66
2ME, exp[a]	$(4.5 \pm 1.4) \times 10^{-12}$	-0.65 ± 0.2
2EE	2.91×10^{-12}	−0.78

[a] From ref 8.

For the •OH + 2EE reaction H abstractions from site 3 were found to be those contributing the most to the overall rate coefficient. Site 3 in 2EE is chemically equivalent to site 2 in 2ME, and both of them are glycol ethers. This similarity is reflected on the branching ratios which behave in the same way for both compounds when reacting with •OH. Therefore the higher reactivity of the site that is α with respect to ether group and β with respect to the alcohol group seems to be a general trend for the glycol moiety. The contribution of path 3 to the overall rate coefficient was found to be 68% at 298 K for 2EE. As the temperature increases such contribution decreases, ranging from 78% at 250 K to 51% at 440 K (Table 4S). Therefore, it can be stated that the influence of temperature on the branching ratios is more significant for glycol ethers than for other hydroxy ethers. As it is the case for 2ME, the branching ratios corresponding to H abstractions from the hydroxyl group in 2EE were found to be negligible. In fact, H abstractions from the OH site were found to contribute to the overall reactions by less than 2% for all the studied hydroxy ethers. This is significantly different than what has been reported for small alcohols.[20,21]

The influence of temperature on the rate of the chemical reactions studied in this work has been interpreted in terms of the Arrhenius equation:[41]

$$k = A\, e^{-E_a/RT} \qquad (14)$$

where A is known as the pre-exponential factor or the frequency factor, and E_a represents the activation energy. In eq 14 the influence of the temperature is accounted for in the exponential part of the expression. Because the Arrhenius equation is probably the most widely used today to interpret kinetic data, it is convenient to use it in the characterization of the rate constants, for comparisons.

The Arrhenius activation energy was found to be negative, in the 250−440 K temperature range for EM, 2ME, and 2EE (Table 8). The only previous report on the temperature Arrhenius parameters for a hydroxy ether reaction with •OH has also been

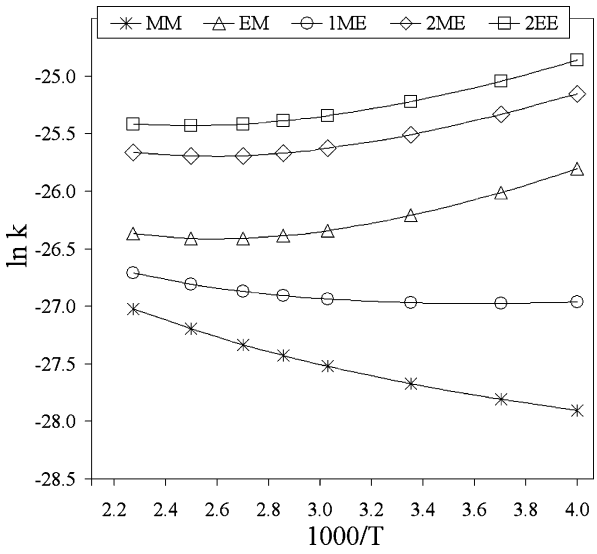

Figure 9. Arrhenius plots for the •OH + hydroxy ethers reactions.

included in Table 8. In that work the fit was performed using the Arrhenius equation; accordingly, we have also fitted the calculated data that way. The agreement between the calculated and experimental data is excellent, supporting the reliability of the presented calculations.

As can be seen in Figure 9, the Arrhenius plots corresponding to the overall reactions are significantly curved for all the studied systems. Consequently, their activation energies change with temperature within the range 250−440 K and the Arrhenius equation is not the best option to describe the influence of temperature on the corresponding rate coefficients. The procedure most commonly used when the plot of ln k vs $1/T$ is not linear is to use the equation proposed by Kooij:[42]

$$k = BT^m \, e^{-E_0/RT} \tag{15}$$

where B, E_0, and m are temperature-independent parameters. This expression is more adequate than eq 14, from both the theoretical and empirical points of view. Even data showing significant deviations from the Arrhenius equation can usually be very well fitted by eq 15. Its applicability can be tested by plotting $\ln(k/T^m)$ vs $1/T$. If a straight line is obtained its slope is equal to $-E_0/R$, and E_0 can be calculated. Differentiation of eq 15 in its logarithmic form leads to:

$$\frac{d \ln k}{dT} = \frac{E_0 + mRT}{RT^2} \tag{16}$$

and comparing eqs 14 and 16, it is clear that the activation energy at each temperature can be calculated as:

$$E_a = E_0 + mRT \tag{17}$$

where E_0 is the hypothetical activation energy at 0 K.

In our case, the plots of $\ln(k/T^m)$ vs $1/T$ yield straight lines, with R^2 almost equal to 1 (the worst value was $R^2 = 0.99996$), proving the applicability of the procedure. The Kooij parameters that best fit the data are shown in Table 9. They were obtained by nonlinear least-squares analysis. Since the starting values are of great importance in such procedure, we have obtained them by following the suggestions in ref 43 for a similar function. We have performed a multiple regression analysis, assuming ln T and $1/T$ as independent variables, since there is no multicollinearity among them, and ln k as the dependent variable. The values of E_0, m, and B obtained that way were then used as the starting values in the nonlinear least-squares analysis, leading to the final values reported in table 9. Since none of the three parameters was fixed and the nonlinear analyses led to R^2 coefficients ≥0.9993, the values obtained here seem to be reliable. In our opinion, the procedure described here is more reliable than that which fixes m, usually using $m = 2$, which can lead to different values of E_0, m, and B, depending on the m value.

TABLE 9: Kooij Parameters for the Studied Reactions between OH Radical and Hydroxy Ethers at the 250−440 K Temperature Range

	B (cm^3 molecule^{-1} s^{-1})	m	E_0 (kcal/mol)
MM	2.35×10^{-20}	2.83	−0.83
EM	3.70×10^{-29}	5.62	−4.30
1ME	5.08×10^{-21}	2.98	−1.65
2ME	3.08×10^{-26}	4.74	−3.67
2EE	6.61×10^{-25}	4.32	−3.45

TABLE 10: Variation of the Activation Energies (kcal/mol) with Temperature, in the 250−440 K Range

T	MM	EM	1ME	2ME	2EE
250	0.58	−1.51	−0.17	−1.32	−1.30
270	0.69	−1.28	−0.05	−1.13	−1.13
298.15	0.85	−0.97	0.11	−0.87	−0.89
330	1.03	−0.61	0.30	−0.57	−0.61
350	1.14	−0.39	0.42	−0.38	−0.44
370	1.25	−0.17	0.54	−0.19	−0.27
400	1.42	0.17	0.72	0.09	−0.01
440	1.64	0.61	0.95	0.47	0.33

It could be interesting to discuss the variation of the activation energy with temperature (Table 10). The overall activation energy increases as temperature rises for all the studied reactions. It is positive in the whole temperature range for the •OH + MM reaction, whereas it change sign for all the other hydroxy ethers. For the •OH reaction with 1ME it is negative from 250 to 270 K and positive for all the other studied temperatures. For EM and 2ME the activation energy become positive only for temperatures above 370 K, whereas for 2EE it was found to be positive only at 440 K.

The analysis of the Kooij parameters is important to interpret apparent negative activation energies. According to the present results, at temperatures close to 298 K this would be the case for 2ME, in agreement with the experimental results,[8] and also for EM, and 2EE predicted here for the first time. According to our calculated Kooij parameters the exponential factor is responsible for such behavior rather than the pre-exponential one. In all cases the temperature dependence of the pre-exponential factor is positive, contrary to what was proposed before.[8] The negative exponent can be justified by the potential energy surfaces of the major channels for the •OH reactions with these three ethers at temperatures close to 298 K. They proceed via prereactant complexes and the apparent enthalpy of activation is negative, in agreement with Singleton and Cvetanovic hypothesis.[13]

According to the values reported in Table 10, in all cases the increase of temperature provokes an increase in the activation energy. This is partially caused by the decrease in the branching ratios of the channels in which transition states are H bonded. Because the rate constants of these channels decrease, or remain almost unchanged, with T, and the k of other channels increase

with T, the overall activation energy would become more dependent on the channels with positive enthalpies of activation as T increases. Therefore, at temperatures higher than 400 K, which is the case of combustion processes, a negative temperature dependence of k it is not expected. We can conclude that for OH radical multichannel H abstraction reactions from oxygenated VOCs the negative temperature dependence is only possible at relatively low temperatures for weak C−H bonds. This is also the case of simple ethers[22] and certainly can be extrapolated to alcohols and probably to aldehydes.

Conclusions

The gas phase reactions of hydroxyl radicals with a series of hydroxy ethers have been studied, taking into account all the possible channels of reaction. The main reaction path was found to involve H abstractions from a C atom located in α position with respect to the ether group for all the studied systems. The presence of H bond interactions in the transition state structures lowers their energy and has a preponderant role on the site reactivity of hydroxy ethers. TSs with seven-member ring-like structures were found to lead to stronger H bond interactions than TSs with six- and five-member ring-like structures, with the latter leading to the weakest interactions. Non-linear Arrhenius plots were found for all the overall reactions, indicating that the activation energy of the studied processes changes with temperature. At 298 K the activation energies of the •OH reactions with EM, 2ME, and 2EE were found to be negative. The influence of temperature on the branching ratios was found to be more significant for glycol ethers than for other hydroxy ethers. The branching ratios corresponding to H abstractions from the hydroxyl group were found to be negligible (<2%). The negative apparent activation energies at relatively low temperatures, found for the reactions of three of the studied systems with the OH radical, can be rationalized assuming a complex mechanism via prereactant complex followed by a H-bonded transition state for the main channel of each reaction. Therefore, the negative temperature dependence is due to apparent negative $\Delta H^{\ddagger}$, not because of negative temperature dependence of the pre-exponential factor. Due to the diverse temperature dependence of different channels, the apparent negative temperature dependence occurs exclusively at relatively low temperatures. The agreement between the calculated and experimental data is excellent, supporting the reliability of the presented calculations and the data provided here for the first time.

Acknowledgment. A. G. thanks Laboratorio de Visualización y Cómputo Paralelo at UAM − Iztapalapa for the access to its computer facilities. J. R. A.-I. thanks the Dirección General de Servicios de Cómputo Académico (DGSCA) at Universidad Nacional Autónoma de México. This work was partially supported by a grant from the DGAPA UNAM (PAPIIT-IN203808).

Supporting Information Available: Optimized geometries of the reactant complexes. Energies of relevant stationary points, relative to isolated reactants. Branching ratios and overall rate coefficients (k) within the 250−440K temperature range. This material is available free of charge via Internet at http://pubs.acs.org.

References and Notes

(1) Guenther, A.; Hewitt, C. N.; Erickson, D.; Fall, R.; Geron, C.; Graedel, T.; Harley, P.; Klinger, L.; Lerdau, M.; McKay, W. A.; Pierce, T.; Scholes, B.; Steinbrecher, R.; Tallamraju, R.; Taylor, J.; Zimmermann, P. *J. Geophys. Res.* **1995**, *100*, 8873.

(2) Guenther, A.; Geron, C.; Pierce, T.; Lamb, B.; Harley, P.; Fall, R. *Atmos. Environ.* **2000**, *34*, 2205.

(3) Sawyer, R. F.; Harley, R. A.; Cadle, S. H.; Norbeck, J. M.; Slott, R.; Bravo, H. A. *Atmos. Environ.* **2000**, *34*, 2161.

(4) Placet, M.; Mann, C. O.; Gilbert, R. O.; Niefer, M. J. *Atmos. Environ.* **2000**, *34*, 2183.

(5) Atkinson, R.; Arey, J. *Chem. Rev.* **2003**, *103*, 4605.

(6) Koppmann, R., Ed. *Volatile Organic Compounds in the Atmosphere*; Blackwell Publishing Ltd.: Oxford, 2007.

(7) Carter, W. P. L. *J. Air Waste Manage. Assoc.* **1994**, *44*, 881.

(8) Dagaut, P.; Liu, R.; Wallington, T. J.; Kurylo, M. J. *J. Phys. Chem.* **1989**, *93*, 7838.

(9) Atkinson, R.; Darnall, K. R.; Lloyd, A. C.; Winer, A. M.; Pitts, J. N., Jr. *Adu. Photochem.* **1979**, *11*, 375.

(10) Logan, J. A.; Prather, M. J.; Wofsy, S. C.; McElroy, M. B. *J. Geophys. Res.* **1981**, *86*, 7210.

(11) Atkinson, R.; Lloyd, A. C. *J. Phys. Chem. Ref. Data* **1984**, *13*, 315.

(12) Atkinson, R. *Chem. Rev.* **1985**, *85*, 69.

(13) Singleton, D. L.; Cvetanovic, R. J. *J. Am. Chem. Soc.* **1976**, *98*, 6812.

(14) (a) Alvarez-Idaboy, J. R.; Mora-Diez, N.; Vivier-Bunge, A. *J. Am. Chem. Soc.* **2000**, *122*, 3715. (b) Alvarez-Idaboy, J. R.; Mora-Diez, N.; Boyd, R. J.; Vivier-Bunge, A. *J. Am. Chem. Soc.* **2001**, *123*, 2018. (c) Mora-Diez, N.; Alvarez-Idaboy, J. R.; Boyd, R. J. *J. Phys. Chem. A.* **2001**, *105*, 9034. (d) Galano, A.; Alvarez-Idaboy, J. R. Atmospheric Reactions of Oxygenated Compounds + OH Radicals: Role of Hydrogen-Bonded Intermediates and Transition States. In *Advances in Quantum Chemistry*; Goodsite, M. E., Johnson, M. S., Eds.; Applications of Quantum Chemistry to the Atmosphere; Elsevier: Amsterdam, 2008; Vol. 55, Ch. 12, p 245. (e) Francisco-Marquez, M.; Alvarez-Idaboy, J. R.; Galano, A.; Vivier-Bunge, A. *Phys. Chem. Chem. Phys.* **2003**, *5*, 1392.

(15) Moriarty, J.; Sidebottom, H.; Wenger, J.; Mellouki, A.; Le Bras, G. *J. Phys. Chem. A* **2003**, *107*, 1499.

(16) Stemmler, K.; Kinnison, D. J.; Kerr, J. A. *J. Phys. Chem.* **1996**, *100*, 2114.

(17) Porter, E.; Wenger, J.; Treacy, J.; Sidebottom, H.; Mellouki, A.; Teton, S.; LeBras, G. *J. Phys. Chem. A* **1997**, *101*, 5770.

(18) Atkinson, R. *Chem. Rev.* **1985**, *85*, 69.

(19) Atkinson, R. *J. Phys. Chem. Ref. Data.* 1994Monograph 2.

(20) McCauley, J. A.; Kelly, N.; Golden, M. F.; Kaufmann, F. *J. Phys. Chem.* **1989**, *93*, 1014.

(21) Galano, A.; Alvarez-Idaboy, J. R.; Bravo-Perez, G.; Ruiz-Santoyo, M. E. *Phys. Chem. Chem. Phys.* **2002**, *4*, 4648.

(22) Zavala-Oseguera, C.; Alvarez-Idaboy, J. R.; Merino, G.; Galano, A. *J. Phys. Chem. A* **2009**, *113*, 13913.

(23) Seakins, P. W. *Annu. Rep. Prog. Chem., Sect. C: Phys. Chem.* **2007**, *103*, 173.

(24) (a) Butkovskaya, N. I.; Kukui, A.; Le Bras, G. *J. Phys. Chem. A* **2004**, *108*, 1160. (b) Butkovskaya, N. I.; Setser, D. W. *J. Phys. Chem. A.* **1999**, *103*, 6921. (c) Butkovskaya, N. I.; Kukui, A.; Pouvesle, N.; Le Bras, G. *J. Phys. Chem. A.* **2004**, *108*, 7021.

(25) , Frisch, M. J.; Trucks, G. W.; Schlegel, H. B.; Scuseria, G. E.; Robb, M. A.; Cheeseman, J. R.; Montgomery, Jr., J. A.; Vreven, T.; Kudin, K. N.; Burant, J. C.; Millam, J. M.; Iyengar, S. S.; Tomasi, J.; Barone, V.; Mennucci, B.; Cossi, M.; Scalmani, G.; Rega, N.; Petersson, G. A.; Nakatsuji, H.; Hada, M.; Ehara, M.; Toyota, K.; Fukuda, R.; Hasegawa, J.; Ishida, M.; Nakajima, T.; Honda, Y.; Kitao, O.; Nakai, H.; Klene, M.; Li, X.; Knox, J. E.; Hratchian, H. P.; Cross, J. B.; Bakken, V.; Adamo, C.; Jaramillo, J.; Gomperts, R.; Stratmann, R. E.; Yazyev, O.; Austin, A. J.; Cammi, R.; Pomelli, C.; Ochterski, J. W.; Ayala, P. Y.; Morokuma, K.; Voth, G. A.; Salvador, P.; Dannenberg, J. J.; Zakrzewski, V. G.; Dapprich, S.; Daniels, A. D.; Strain, M. C.; Farkas, O.; Malick, D. K.; Rabuck, A. D.; Raghavachari, K.; Foresman, J. B.; Ortiz, J. V.; Cui, Q.; Baboul, A. G.; Clifford, S.; Cioslowski, J.; Stefanov, B. B.; Liu, G.; Liashenko, A.; Piskorz, P.; Komaromi, I.; Martin, R. L.; Fox, D. J.; Keith, T.; Al-Laham, M. A.; Peng, C. Y.; Nanayakkara, A.; Challacombe, M.; Gill, P. M. W.; Johnson, B.; Chen, W.; Wong, M. W.; Gonzalez, C.; Pople, J. A.; *Gaussian 03, Revision E.01*; Gaussian, Inc.: Wallingford CT, 2004.

(26) As implemented in Gaussian 03: $0.5E_X^{HF} + 0.5E_X^{LSDA} + 0.5\ddot{a}E_X^{Becke88} + E_C^{LYP}$.

(27) (a) Cizek, J. *Adv. Chem. Phys.* **1969**, *14*, 35. (b) Purvis, G. D.; Bartlett, R. J. *J. Chem. Phys.* **1982**, *76*, 1910. (c) Scuseria, G. E.; Janssen, C. L.; Schaefer III, H. F. *J. Chem. Phys.* **1988**, *89*, 7382. (d) Scuseria, G. E.; Schaefer III, H. F. *J. Chem. Phys.* **1989**, *90*, 3700.

(28) See for example: (a) Alvarez-Idaboy, J. R.; Galano, A.; Bravo-Pérez, G.; Ruiz-Santoyo, M. E. *J. Am. Chem. Soc.* **2001**, *123*, 8387. (b) Alvarez-Idaboy, J. R.; Cruz-Torres, A.; Galano, A.; Ruiz-Santoyo, M. E. *J. Phys. Chem. A.* **2004**, *108*, 2740. (c) Galano, A.; Alvarez-Idaboy, J. R.; Ruiz-Santoyo, M. E.; Vivier-Bunge, A. *Chem. Phys. Chem.* **2004**, *5*, 1379. (d) Galano, A.; Alvarez-Idaboy, J. R.; Ruiz-Santoyo, M. E.; Vivier-Bunge,

A. *J. Phys. Chem. A.* **2005**, *109*, 169. (e) Galano, A.; Cruz-Torres, A.; Alvarez-Idaboy, J. R. *J. Phys. Chem. A* **2006**, *110*, 1917.

(29) Szori, M.; Fittschen, C.; Csizmadia, I. G.; Viskolcz, B. *J. Chem. Theory Comput.* **2006**, *2*, 1575.

(30) Gonzalez, C.; Schlegel, H. B. *J. Phys. Chem.* **1990**, *94*, 5523.

(31) Gonzalez, C.; Schlegel, H. B. *J. Chem. Phys.* **1989**, *90*, 2154.

(32) Eyring, H. *J. Chem. Phys.* **1935**, *3*, 107.

(33) Evans, M. G.; Polanyi, M. *Trans. Faraday Soc.* **1935**, *31*, 875.

(34) Truhlar, D. G.; Hase, W. L.; Hynes, J. T. *J. Phys. Chem.* **1983**, *87*, 2664.

(35) Eckart, C. *Phys. Rev.* **1930**, *35*, 1303.

(36) Alvarez-Idaboy, J. R.; Galano, A. *Theor. Chem. Acc.* **2010**, *126*, 75.

(37) Robinson, P. J.; Holbrook, K. A.; *Unimolecular Reactions*; Wiley-Interscience: London, 1972.

(38) (a) Yamada, T.; Taylor, P. H.; Goumri, A.; Marshall, P. *J. Chem. Phys.* **2003**, *119*, 10600. (b) Gonzalez-Lafont, A.; Lluch, J. M. *J. Mol. Struct. THEOCHEM* **2004**, *709*, 35.

(39) Masgrau, L.; Gonzalez-Lafont, A.; Lluch, J. M. *J. Phys. Chem. A* **2002**, *106*, 11760.

(40) Alvarez-Idaboy, J. R.; Cruz-Torres, A.; Galano, A.; Ruiz-Santoyo, M. E. *J. Phys. Chem. A.* **2004**, *108*, 2740.

(41) Arrhenius, S. *Z. Phys. Chem.* **1889**, *4*, 226.

(42) Kooij, D. M. *Z. Phys. Chem.* **1893**, *12*, 155.

(43) Draper, N. R.; Smith, H.; *Applied Regression Analysis*; John Wiley & Sons, Inc.: New York, 1966; Ch. 10, p 458.

JP103575F